Electronic Supplementary Material (ESI) for Journal of Materials Chemistry A.

Supporting Information

Unprecedented Plasmon-Induced Nitroxide-Mediated Polymerization (PI-NMP): a Method for Preparation of Functional Surfaces

Olga Guselnikova[a,b], Sylvain Marque[c §], Evgeny Tretyakov[d,e §], David Mares[f], Vitezslav Jerabek[f], Gérard Audran[c], Jean-Patrick Joly[c], Marina Trusova[b], Vaclav Svorcik[a], Oleksiy Lyutakov [a,b], Pavel Postnikov[a,b]

Abstract

A plasmon as a stimulus opens up new opportunities for selective and regulated “from-surface” polymerization and functionalization of surfaces. Here, the first example of plasmon-assisted nitroxide-mediated polymerization (NMP) of stimuli-responsive block copolymers poly(N-isopropylacrylamide)-co-4-vinylboronic acid is reported. The growth of polymer film at room temperature was achieved via plasmon-induced homolysis of alkoxyamines covalently attached to the surface of plasmon-active gold gratings at room temperature. Control of temperature, finite-difference time-domain method simulation of plasmon intensity distribution shift during polymerization, electron paramagnetic resonance experiments and other assays provide strong support for the plasmon-initiated mechanism of NMP. We demonstrated not only the control of resulting polymer thickness but also the preparation of a Surface-enhanced Raman spectroscopy chip for detection of glycoproteins as a powerful example of plasmon-assisted NMP potential.

Table of Contents

Experimental Procedures

General remarks

^{1}H NMR spectra were recorded on Bruker Avance III™ (500 MHz) spectrometer. Chemical shifts are given in parts per million (δ/ppm), referenced to dimethylsulfoxide (2.51) as internal standards. All coupling constants are absolute values and are expressed in Hertz (Hz). The description of signals include: s = singlet, d = doublet. ^{13}C NMR spectra were recorded on Bruker Avance III™ (500 MHz) spectrometers. Routine monitoring of reactions was performed using silica gel coated aluminum plates (Merck, silica gel 60, F_{254}) which were analyzed under UV-light at 254 nm and dipped into a solution of 2-naphthol (5 % naphthol in 10 % NaOH aqueous, dipping solution). Solvent mixtures are understood as volume/volume. Solvents, reagents, and chemicals were purchased from Sigma/Aldrich. Solvents, reagents, and chemicals were used as purchased unless stated otherwise.

Materials

Acetic acid (reagent grade, ≥99 %), diethyl ether, deionized water, p-Toluenesulfonic acid monohydrate (ACS reagent, ≥98.5 %), N-Isopropylacrylamide (≥99%), 4-Vinylphenylboronic acid (≥95%), 1,2-Dihydroxybenzene (ReagentPlus®, ≥99%), Dichloromethane (anhydrous, ≥99.8%), high-purity water (EMD MILLIPORE), Acetone (≥99.9%), Ethanol (analytical standard) were purchased from Sigma-Aldrich and used without further purification.

Samples preparation

Grating preparation.

Briefly, deposited by spin-coating Su-8 thin films were irradiated by excimer laser (3500 laser pulses, 9 mJ cm^{-2} laser fluencies) to create the polymer grating. The Au was deposited onto a patterned polymer surface by vacuum sputtering (discharge power of 7.5 W, sputtering time 200 s, resulted in thickness 25 nm) [S1]

*Preparation of alkoxyamine initiator **(1)**.*

Alkoxyamine initiator was prepared according to [S2].

*Electrografting of alkoxyamine initiator **(1)**.*

Modification of gold grating by electrochemical reduction of in situ generated diazonium was carried out in a mixture of water and methanol (1/1) at room temperature. To a solution of p-TsOH (0.14 g, 0.5 mmol) in methanol (2 mL), tert-butyl nitrite was slowly added (60 µL, 0.5 mmol). Next, the aniline derivative of alkoxyamine initiator (**1**) 0.013 g, 0.3 mmol) was added in 4 steps to the reaction mixture over 1 min. The mixture was left to react for about 40 min prior to the electrochemical functionalization. After 2 ml of water was added to the reaction mixture and left to 10 minutes. Electrografting of gold gratings was performed in a resulting solution of corresponding diazonium salts without the addition of any electrolytes under the potential –2 V for 10 min with a platinum counter electrode. After modification metal substrates were rinsed under sonication sequentially with deionized water, ethanol, and acetone for 10 min and dried in a desiccator for 3 hours.

Plasmon-induced NMP polymerization.

Polymerization was performed in a glass petri dish in the air using portable ProRaman-L spectrometer (785 nm) with the laser power density of 10 µW/µm^2. Every time before starting the process, spectra of the modified gold surface was recorded. For the plasmon-induced NMP, the gold grating grafted with (**1**) were firstly immersed in the 10 mM solution of monomer (NIPAM or VBA) and after illuminated for a definite time. After polymerization, gold substrates were rinsed sequentially with dichloromethane, methanol, and acetone under sonication to remove any unreacted monomers. Raman spectra were measured 30 times, each of them with 3 s accumulation time.

Measurement techniques

The X-ray photoelectron spectroscopy (XPS) was performed using an Omicron Nanotechnology ESCAProbeP spectrometer fitted with monochromated Al K Alpha X-ray source working at 1486.6 eV. For characterization of the sample surface morphology, the peak force AFM technique was applied using the Icon (Bruker) microscope. Raman scattering was measured on portable ProRaman-L spectrometer (Laser power 15 mW) Raman spectrometer with 785 nm excitation wavelength. Spectra were measured 30 times, each of them with 3 s accumulation time.

SERS sensing of catechol.

PNIPAM/VBA grafted gold gratings were immersed in aqueous solution of in aqueous solutions of catechol at pH 7.4 in concentrations 10^{-8} M rapidly heated above LCST (35°C) for 5 min, washed with the hot water, cooled down to room temperature and dried on air. For room temperature measurements, gold gratings were immersed in the catechol solution without heating (23°C) and dried on air.

SERS sensing of α-1 acid glycoprotein.

PNIPAM/VBA grafted gold gratings were immersed in aqueous solution of in PBS solutions of α-1 acid glycoprotein at pH 7.4 in concentrations 10^{-8} M rapidly heated above LCST (35°C) for 5 min, washed with the hot water, cooled down to room temperature and dried on air. For room temperature measurements, gold gratings were immersed in the catechol solution without heating (23°C) and dried on air.

Simulation Techniques.

The excitation of surface plasmon-polariton (SPP) on noble grating surface was simulated using the RSoft photonic simulation suite using the rigorous and fully vectoral solution of Maxwell's equations in periodic structures. Rigorous Coupled Wave Analysis algorithm enhanced with Modal Transmission Line was applied.

EPR measurements.

A gold plate of 0.5x1 cm^2 grafted by alkoxyamine initiator was immersed in 3 ml of DCM and irradiated by laser at 780 nm with the 10 µW/µm^2 power for 60 min. The resulting solution was evaporated to dry and residue solved in 0.3 mL of tert-Butylbenzene as a solvent. The concentration of released nitroxide was estimated using X-band EPR Bruker machine with following parameters: receiver gain at 10E4, modulation amplitude at 2G, sweep time at 21 s, sweep width at 200G, and power at 20 mW. As a reference, 0.1 mM solution of TEMPO (0.3 mL) was used to determine the amount of radical species. Blank experiment with alkoxyamine was performed in the same conditions (90 minutes irradiation) and no generation of nitroxide was observed.

Temperature control experiments.

The gold gratings grafted with initiator was placed in the petri dish and the ultrathin leaf-type thermocouple (Thomas Traceable® Waterproof Type K Thermometer probe) was attached to the sample surface and fixed using the thermo-conductive paste. The laser beam (780 nm) was focused on the sample surface close to the working edge of the thermocouple, and the temperature changes were monitored during the reaction process. The temperature-control experiments were performed in the reaction mixture solution (NIPAM dissolved in DCM). The (independent/separated/simultaneous) measurement of DCM solution temperature was also performed using a second thermocouple (Thomas Traceable® Waterproof Type K Thermometer probe) placed in the solution at the 0.2 cm distance from the illuminated place.

Preparation and properties of gold gratings

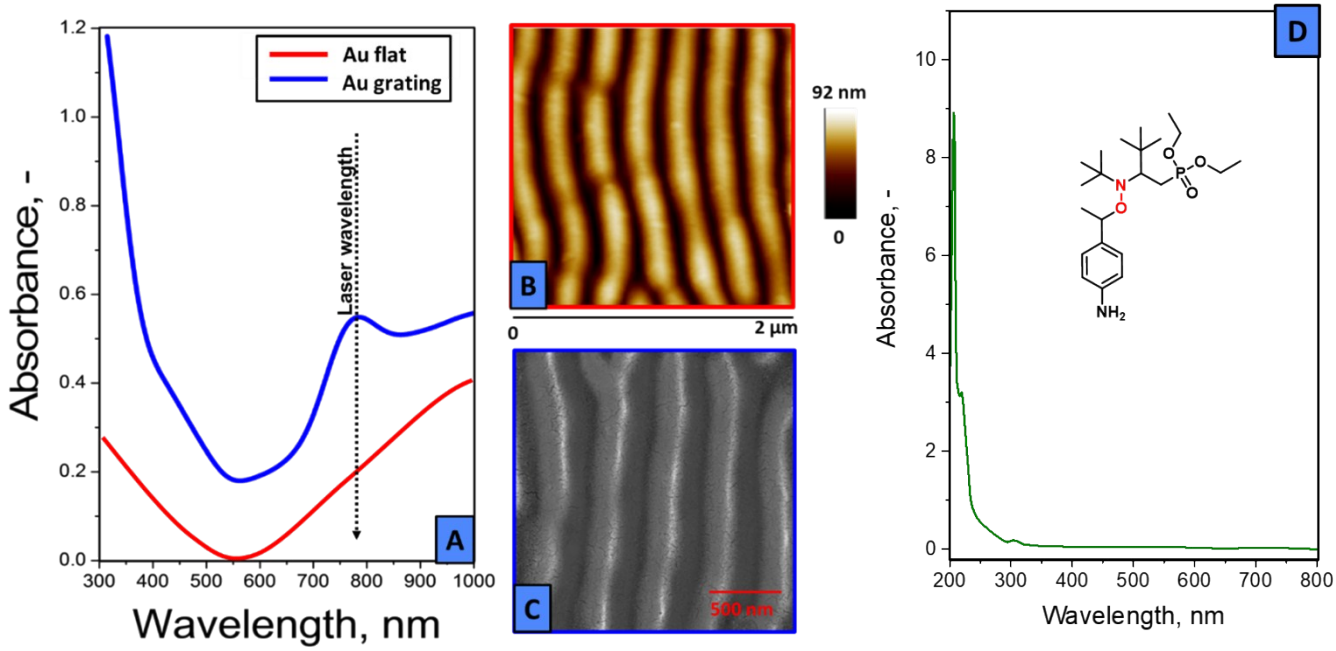

Fig. S1. (A) UV spectra, (B) AFM morphology image, (C) SEM image of Au grating, (D)-UV spectra of **1**

Grafting of alkoxyamine initiator

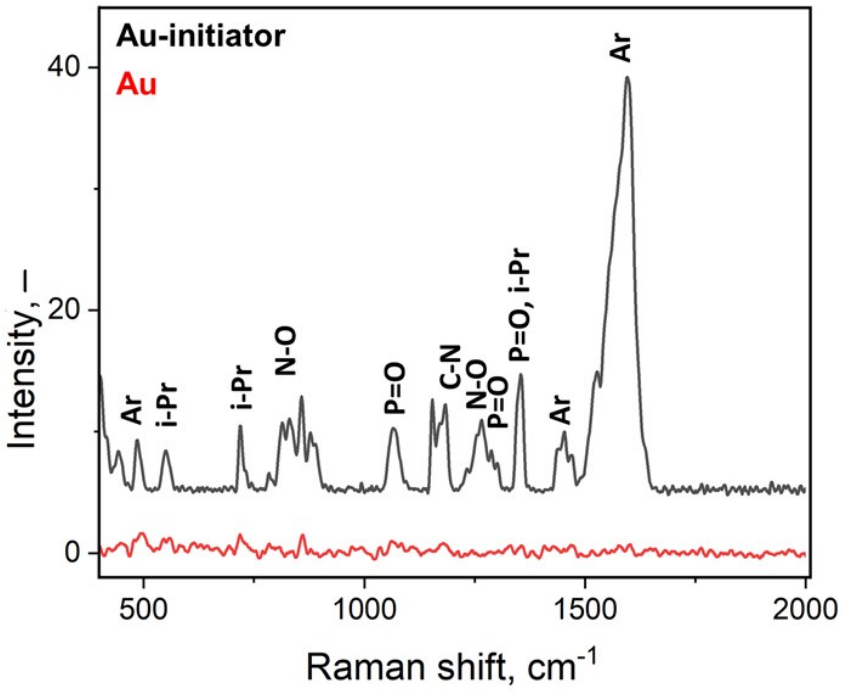

Fig. S2. Raman spectra of gold grating before and after grafting of alkoxyamine initiator.

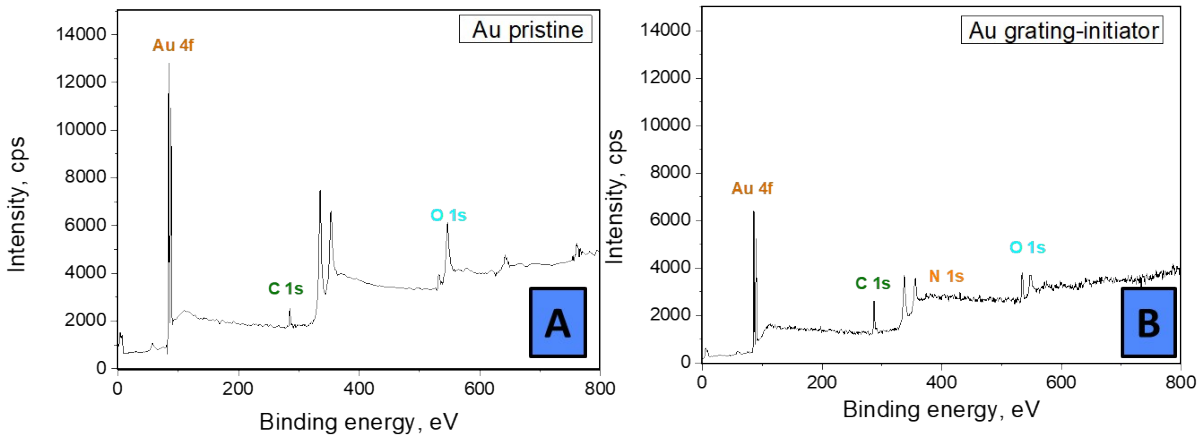

Fig. S3. XPS survey spectra of (A) pristine gold, (B) after covalent grafting of the initiator.

Table S1. Surface Atomic concentration according to XPS of pristine gold, after grafting of initiator, after 60 min of polymerization of NIPAM under sunlight, after 30 and 60 min of polymerization of NIPAM under 780 nm, after 30 min of polymerization of NIPAM and 30 min of polymerization of VBA under 780 nm irradiation light.

Sample	**Atomic concentration (%)**				
	C	**N**	**Au**	**O**	**B**
Au Grating Pristine	35.9	-	69.1	25.7	-
Au-initiator	41.2	2.0	38.3	18.5	-
Au Grating sun light	59.2	4.7	21.6	14.5	-
Au Grating PNIPAM 780 nm, 30 min	63.1	6.8	12.5	17.6	-
Au Grating PNIPAM 780 nm, 60 min	68.4	9.1	1.7	20.8	-
Grating 30 min PNIPAM 30 min VBA 780 nm	65.5	6.9	1.1	23.3	3.2

Confirmation of initiator covalent grafting by in situ diazotation/modification

Chemical modification of gold gratings was confirmed using the Raman and XPS spectroscopies. The Raman spectra of the pristine gold film do not show any significant peaks (Fig. S2), while electrochemical modification introduces specific Raman peaks. After grafting of Initiator molecules following Raman bands appear: 1594, 1452 (Ar ring), 1350 (P=O stretch, i-Pr vibrations), 1260 (N–O vibrations), 1184, 1150 (C-N stretch), 1070 (P=O stretch), 890–812 (N–O stretch), 720, 550 (Alkyl vibrations), 490 cm^{-1} (Ar ring).

Fig. S3 shows the XPS spectra taken on the pristine and grafted with initiator groups via diazonium modification gold surfaces. The elements' concentrations, calculated from XPS spectra, are listed in the Tab. S1. The pristine Au surface shows peaks related to Au 4f (84.3 eV), C 1s (287.2) and O1s (532 eV). Electrografting with initiator results in the apparent increase of carbon concentration to 5.3 %, the raise of Ns 1s peak at 401.2 eV, and the increase of O1s peak at 534.8 eV (responsible for C-O bond), typical for nitroxides [S3] simultaneously with the decrease of Au-relate XPS peak. So, the combination of XPS and Raman spectroscopy results clearly confirm the surface modification of gold gratings.

Calculation of thickness by XPS

The thickness of organic (grafted alkoxyamine, later polymer) film was estimated from the surface chemical composition and signal intensities reported in Table S1 and Fig. S3 according to [S4]. We observed gold signal (Au $4f_{7/2}$ is chosen, 84.3 eV) attenuation after modification due to attachment of alkoxyamine (later polymer) and covering of surface. Attenuation of the gold related signal was used for calculation of organic layer thickness using the following equation:

$I/I_0 = \exp(-d/\lambda \sin\theta)$,

d - layer thickness,

λ - mean free path of photoelectron in the organic layer,

θ - the analysis takeoff angle relative to the surface (90° form plain surface),

I/I_0 - the ratio of the Au$4f_{7/2}$ peak intensities (initiator modified surface/bare surface=7687/12829) .

The value of λ was deduced from the empirical formula derived by Seah and Dench [S5, S6]

$\lambda_k = A_n/E_k^2 + B_nE_k^{1/2}$, where E_k is the kinetic energy of photoelectrons.

For an Al Kα source $E_k = 1486.6 - E_B = 1486.6 - 84.3 = 1401.7$ eV

If the substrate is coated with organic materials, $A_n = 49$ and $B_n = 0.11$, the unit of λ is mg/m^2, and the unit of energy is the electron volt.

$\lambda_k = A_n/E_k^2 + B_nE_k^{1/2} = 49/(1401.7)^2 + 0.11*(1401.7)^{1/2} = 0.00296\ mg/m^2$

To convert λ into nanometer units, it has to divide λ in mg/m^2 by the density of the overlayers, approximately assumed here to be equal to 1.0 g/cm^3. For Au4f7/2, λ_k is calculated to be 4.12 mg/m^2 and thickness is found to be 2.1 nm.

The surface coverage for gold grating grafted with initiator film was also calculated according to formula (molar weight is 437 g/mol):

$$\Gamma_{initiator} = \frac{Na * \rho * d}{M} = \frac{6.02 * 10^{23} * 1 * 2.1}{437 * 10^{21}} = 2.8 \frac{molecules}{nm^2}$$

Grafting of PNIPAM film to the gold grating

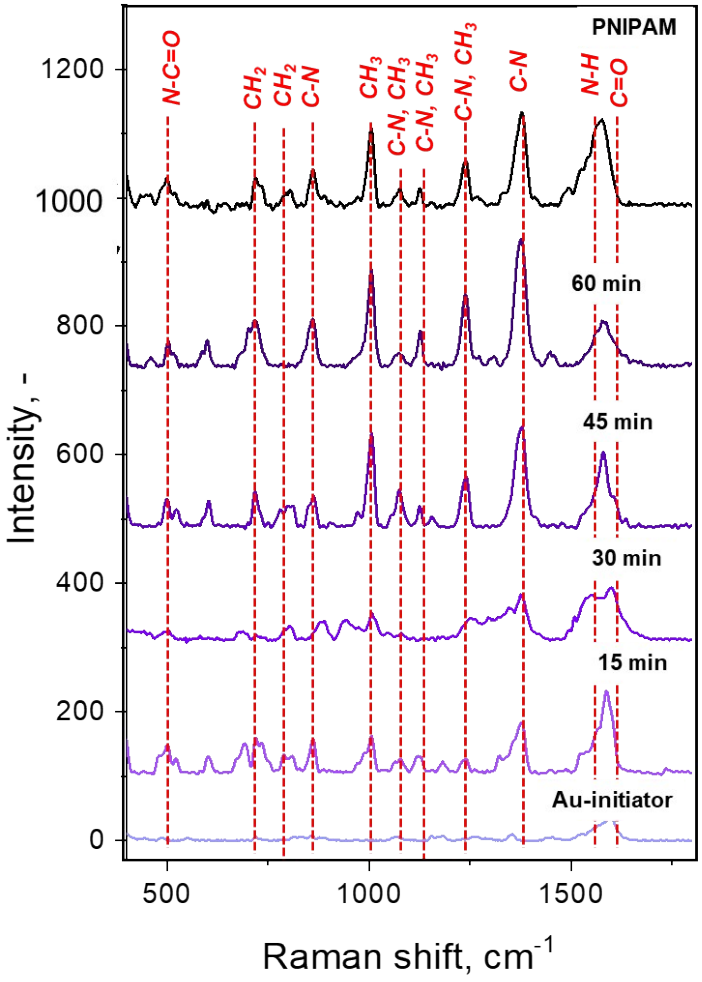

Fig. S4. Time-dependent SERS spectra of plasmon-induced NMP polymerization of PNIPAM on gold gratings.

The growth of PNIPAM film on the gold grating

Bottom and top spectra (in the Fig. 4) display the signal spectrum of grafted initiator **3** and typical Raman response of pristine PNIPAM (measured in "bulk", using the polymer control sample). The other spectra display SERS signals corresponding to a time-dependent surface from PNIPAM grafting. Comparison of the bottom and top SERS spectra indicates that there are several Raman bands, which are ascribed solely to PNIPAM: 513 (N–C=O), 742, 758 (CH_2 stretch), 812 (C–N stretch), 1000 (CH_3 vib), 1082, 1104, 1370 (C–N, CH_3 vib) and formation of amide bonds 1552, 1623 cm^{-1}.

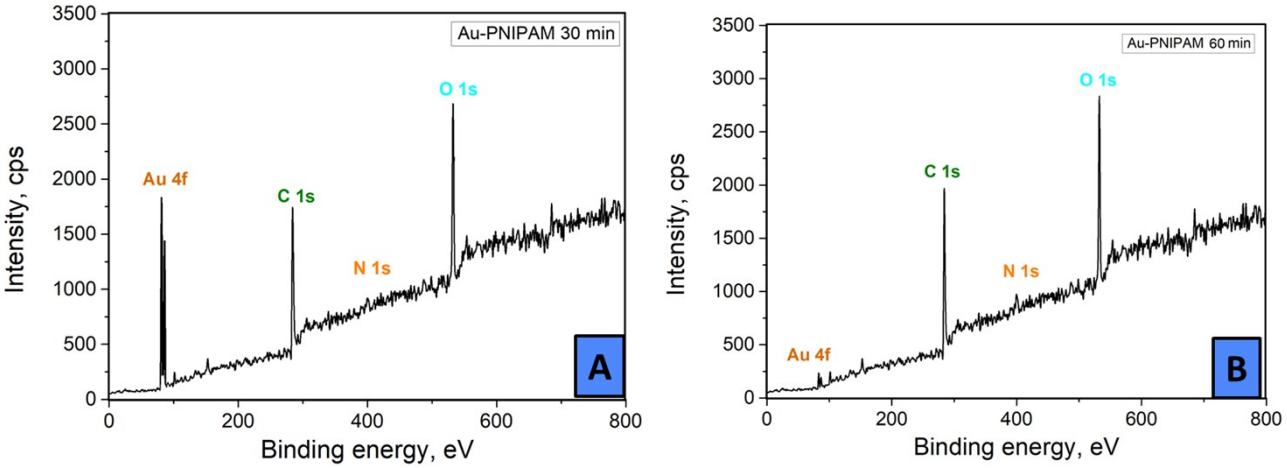

Fig. S5. XPS survey spectra of gold grating surface: (A) after 30 min polymerization with NIPAM, (B) after 60 min polymerization with NIPAM.

In the same way, the thickness of grafted PNIPAM (30 min, 780 nm) can be calculated taking into consideration the density 1.1 g/cm^3 and was found to be 7.32 nm, $\Gamma_{PNIPAM\text{-}30} = 43.07 \frac{molecules}{nm^2}$, and after 60 min of NIPAM polymerization the thickness of grafted PNIPAM can be calculated taking into consideration the density 1.1 g/cm^3 and was found to be 16.9 nm, $\Gamma_{PNIPAM\text{-}60} = 99.04 \frac{molecules}{nm^2}$ as we assumed a controlled growth of polymer chains on the grafted NMP initiator, 35-unit chain length was reached after 60 minutes of irradiation.

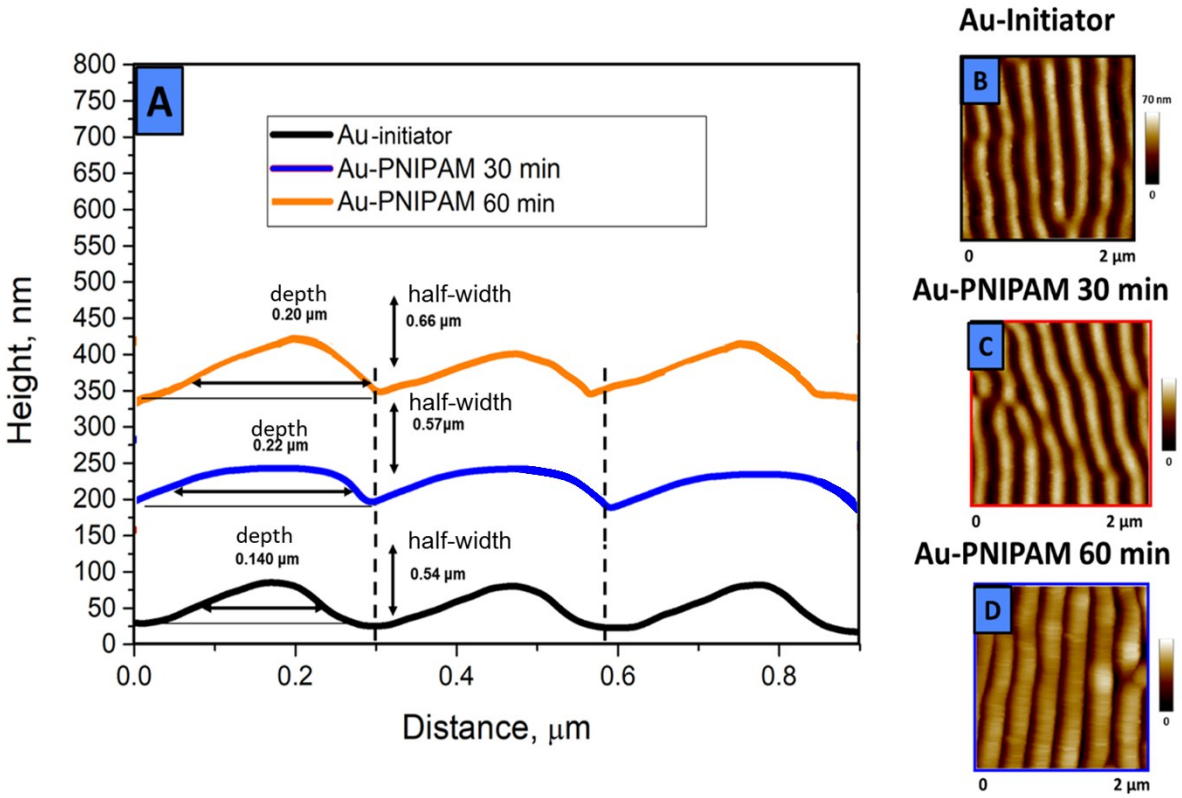

Fig. S6. AFM profile of gold grating modified by 2, after 30 min of NIPAM polymerization and after 30 min of VBA polymerization and corresponding AFM images (B, C, D).

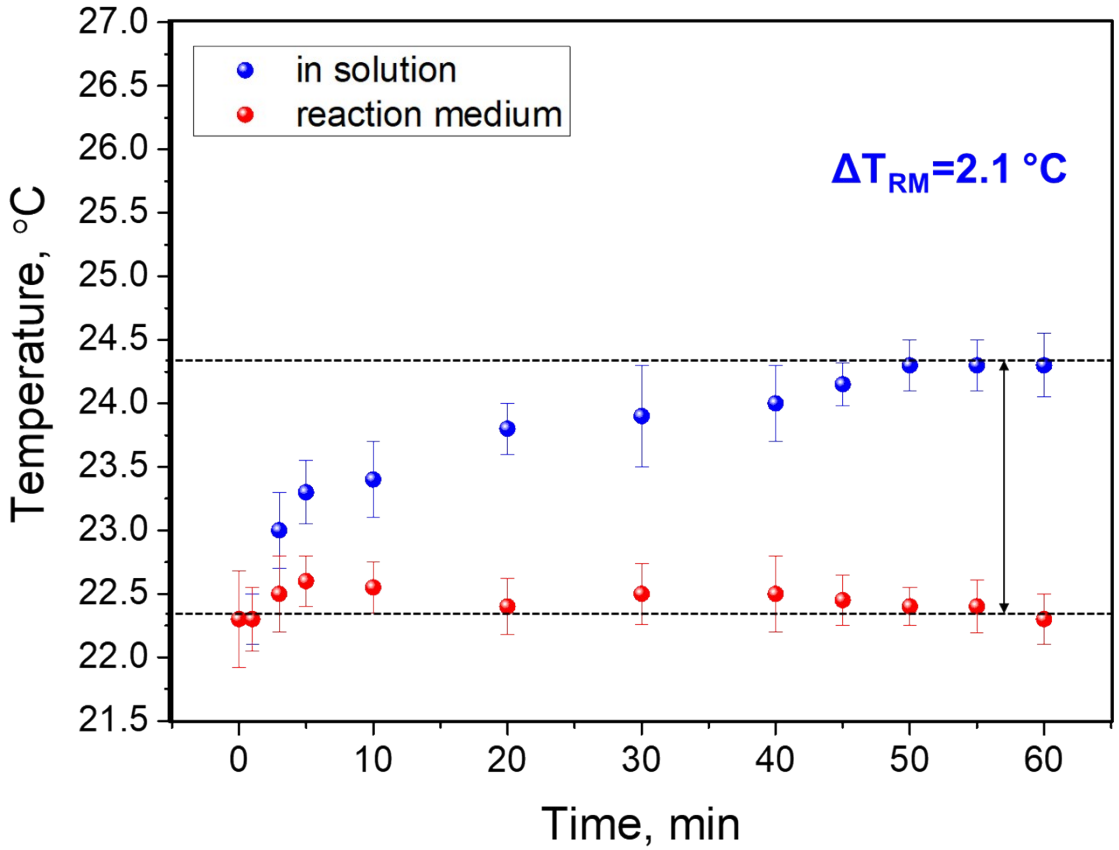

Fig. S7 Temperature changes due to plasmonic heating as a function NMP polymerization time, measured in reaction solution.

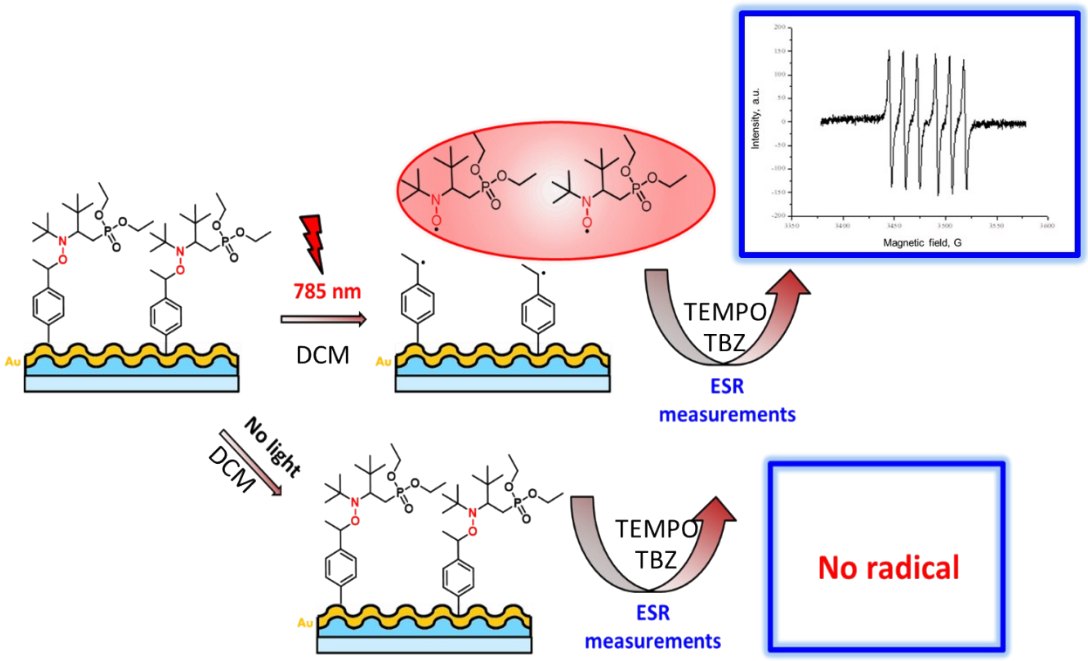

Fig. S8. ESR measurements.

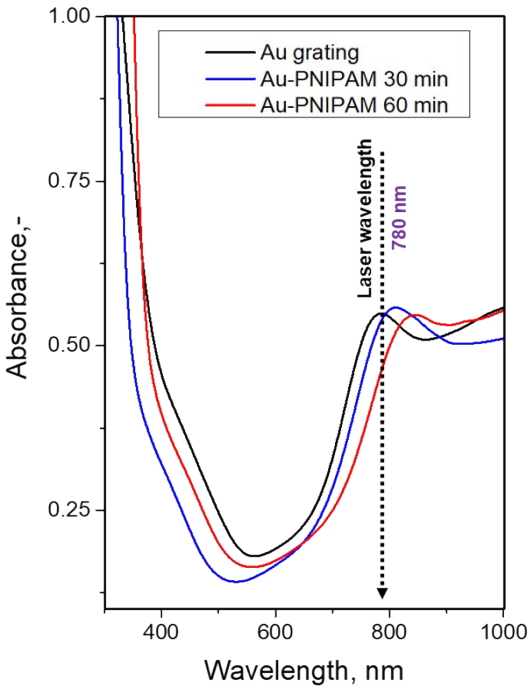

Fig. S9 UV spectra of gold grating and gratings after 30 and 60 min of plasmon-induced polymerization of NIPAM

Grafting of VBA film to the gold grating

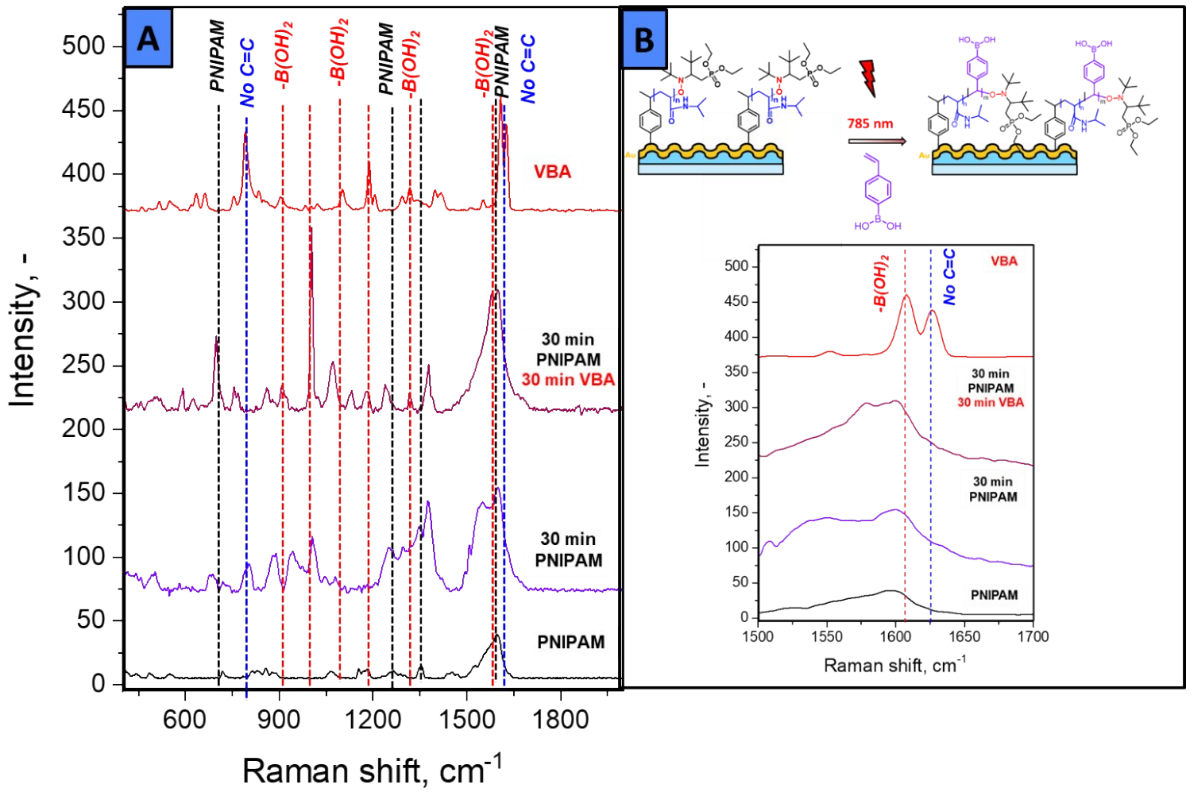

Fig. S10. (A) Time-dependent SERS spectra of plasmon-induced NMP polymerization of VBA on gold gratings with grown PNIPAM, (B) scheme of plasmon-induced polymerization of VBA and an enlarged region of SERS spectra.

The growth of VBA film of the gold grating grafted with PNIPAM

Bottom and top spectra (Fig. S10) display the signal of grafted for 30 min PNIPAM and typical Raman response of pristine VBA (measured in "bulk", using the polymer control sample). In the resulting spectra after VBA grafting, we observed the conservation of PNIPAM-related peak simultaneously with the raise of a new peak at 910, 987, 1074, 1378 and 1584 cm^{-1} corresponding to -$B(OH)_2$ functional groups. Moreover, there is no peak of C=C from a monomer, indicating that appeared peaks are due to the formation of a covalent bond, not physical adsorption.

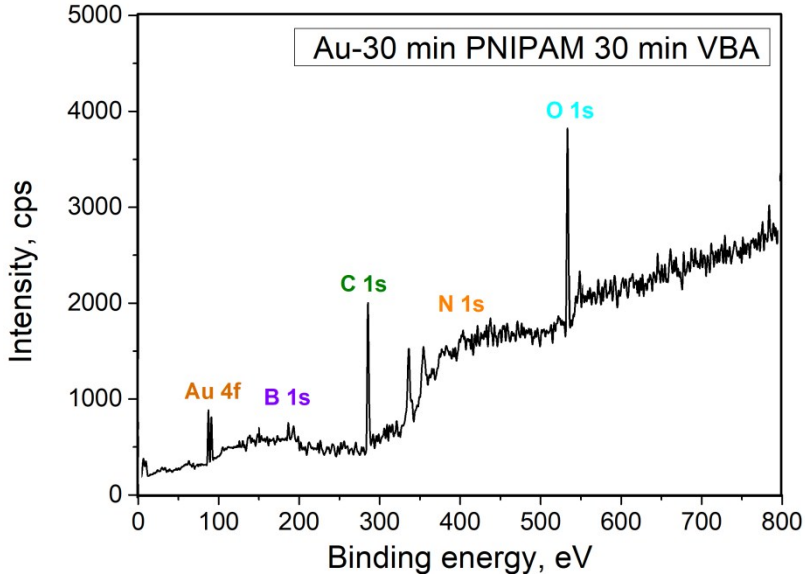

Fig. S11. XPS survey spectra of gold grating after 30 min polymerization with NIPAM and 30 min with VBA.

In the same way, as described above, the thickness of grafted VBA (PNIPAM 30 min, VBA 30 min) can be calculated taking into consideration the volume masses 1.078 g/cm^3 and was found to be 14.7 nm, $\Gamma_{PNIPAM\text{-}VBA} = 85.14 \frac{molecules}{nm^2}$.

As we assumed a controlled growth of polymer chains on the grafted NMP initiator, we suppose than after 30 min irradiation 15.4 monomer unit, while further illumination in the presence of VBA leads to the growth of 15 units more of VBA.

SERS detection of catechol

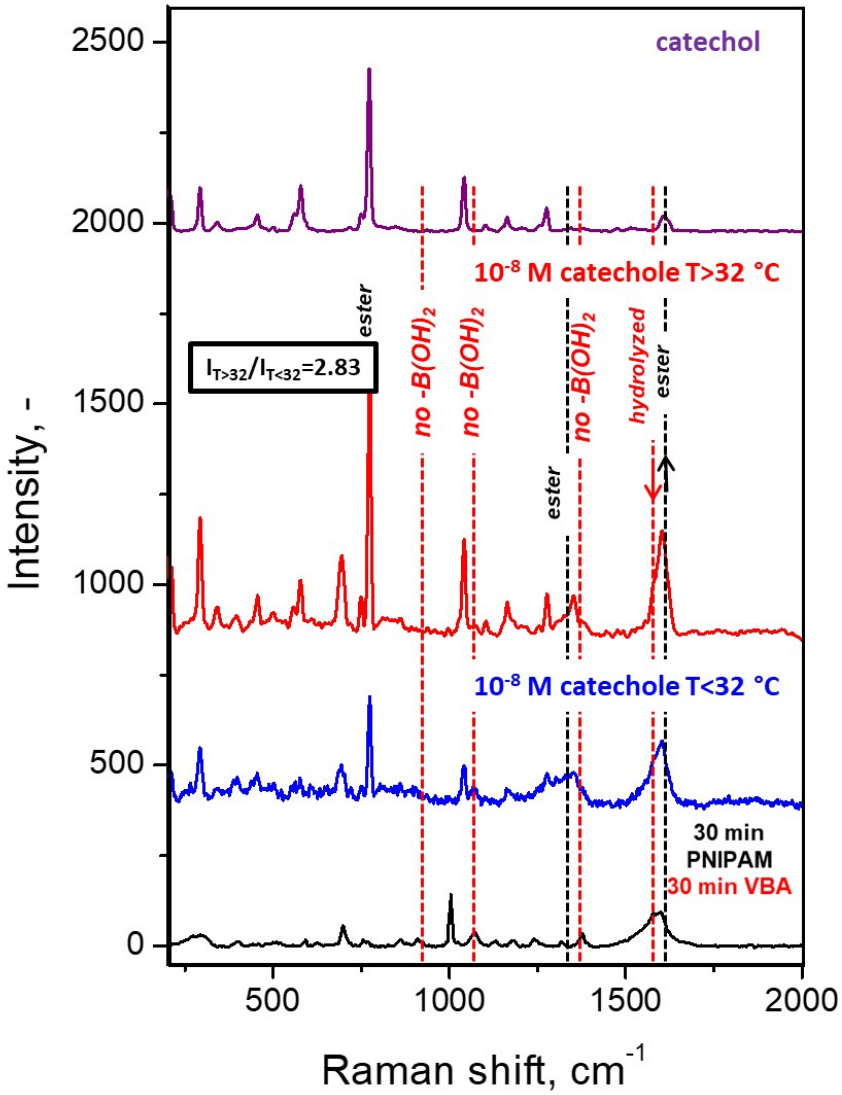

Fig. S12. SERS detection of catechol (10^{-8} M aqueous at pH 7.4).

After the interaction of Au-PNIPAN/VBA gratings with a solution of catechol, we observed considerable changes in the spectra, responsible for the vibrations formed between VBA and catechol ester, allowing detection of catechol. The significant changes are also attributed to the disappearance of B-$(OH)_2$ groups at 910, 1074 and 1387 cm^{-1}. We also observed an increase of peak at 1600 cm^{-1} simultaneously with a decrease of peak intensity at 1584 cm^{-1}, demonstrating the formation of ester consistently with [S7, S8]. The changes of SERS spectra after immersion of sample on catechol solution is well-visible due to the VBA moieties on the gold surface, however, capturing of the analyte at an elevated temperature above LCST of PNIPAM lead to the signal amplification in 2.83 times, potentially increasing the limit of detection.

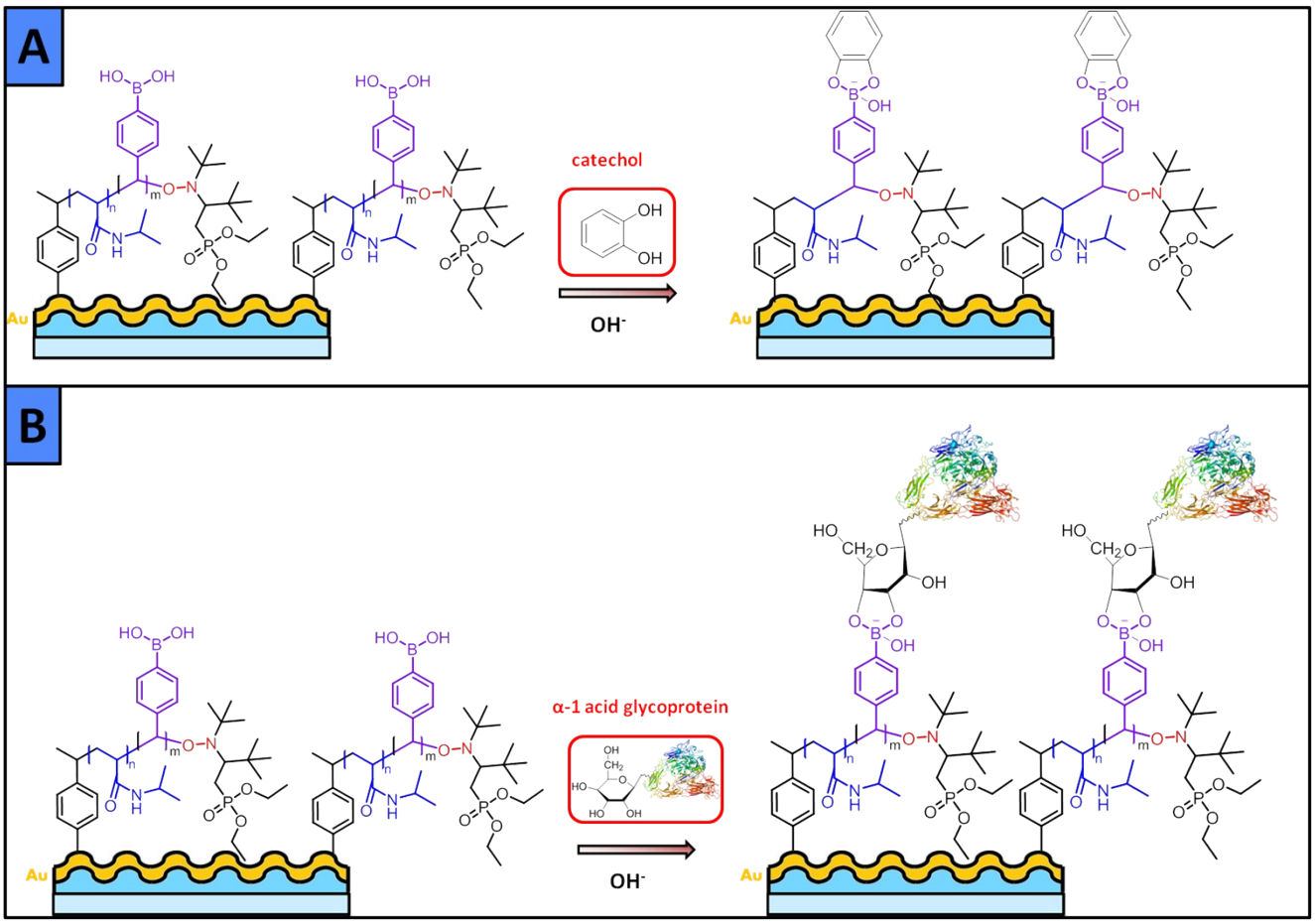

Fig. S13. Recognition mechanism toward (A) catechol and (B) α-1 acid glycoproteins at pH 7.4 on the gold grating grafted with PNIPAM and VBA.

SERS detection of catechol α-1 acid glycoprotein

After interaction of Au-PNIPAN/VBA gratings with a solution of α-1 acid glycoprotein, we observed the disappearance of -B-$(OH)_2$ peaks at 910, 1074 1378 cm^{-1} as in case of catechol. Moreover, we observed appearance of peak corresponded to the α-1 acid glycoprotein at 496 (S–S vib), 674 (C–S str), 1116 (C–C/C–N vib), and 1375 (C(=O)–O vib), which are consistent with [S10]. We also observed an increase of peak at 1602 cm^{-1} simultaneously with a decrease of peak intensity at 1587 cm^{-1}, demonstrating the formation of ester consistently with [S9].

References

[S1] Y. Kalachyova, D. Mares, V. Jerabek, P. Ulbrich, L. Lapcak, V. Svorcik, O. Lyutakov, *Phys. Chem. Chem. Phys.* **2017**, 19(22), 14761–14769.

[S2] G. Audran, P. Brémond, J. P. Joly, S. R. Marque, T. Yamasaki, *Org. Biomol. Chem*. **2016**, 14(14), 3574–3583.

[S3] Y. Shen, Y. Wang, J. Chen, H. Li, Z. Li, C. Li, *J. App. Pol. Sci.* **2010**, 118(2), 1198–1203.

[S4] H. Gehan, L. Fillaud, M. M. Chehimi, J. Aubard, A. Hohenau, N. Felidj, C. Mangeney, *ACS Nano* **2010**, 4(11), 6491–6500.

[S5] D. Briggs, M. P. Seah, In Practical Surface Analysis: Auger and X-Ray Photoelectron Spectroscopy, 2nd ed.; JohnWiley: Chichester, U.K. **1990**, 1, 209.

[S6] J. Pinson, F. Podvorica, *Chem. Soc. Rev.* **2005**, 34, 429–439.

[S7] D. Xie,W. F. Zhu, H. Cheng, Z. Y. Yao, M. Li, Y. L. Zhao, *Phys. Chem. Chem. Phys.* **2018**, 20, 8881–8886.

[S8] X.-H. Pham, S. Shim, T.-H. Kim, H. Hahm, H.- M. Kim, W.-T. Rho, D. H. Jeong, Y.-S. Lee, B. -H. Jun, *BioChip J* **2017**, 11(1), 46–56.

[S9] V. Kopecký, R. Ettrich, K. Hofbauerová, V. Baumruk, *Biochem. Biophys. Res. Comm.* **2003**, 300(1), 41–46.